



OPEN Foliar image-based characterization of airborne particulate matter in an urban area and its implications for remediation

Ankesh Tiwari^{1,9}, Triratnesh Gajbhiye², Mohineeta Pandey¹, Kajal Agrawal¹, Shuvadashini Naik¹, Shubhrasmita Meher¹, Dinesh Patel¹, Rashmi Dubey³✉, Tanzil Gaffar Malik^{1,4}, Mohammed Zari⁵, Ali Zari^{6,7,10}, Khalid M Alghamdi⁶, Khalid Rehman Hakeem^{6,7,8,10,11} & Sudhir Kumar Pandey¹✉

This study addresses the pervasive issue of particulate matter (PM) emission in urban areas, proposing a better approach using scanning electron microscope (SEM) techniques to identify plant species effective in airborne PM removal. Conducted in Bilaspur city, the research strategically selected six plant species across four distinct sites and applied the SEM-Image J method for analysis, yielding significant insights, especially in the respirable PM range. Among the tested plant species, *Senna siamea* and *Dalbergia sissoo* emerged as consistent and standout performers, displaying the highest PM removal efficiency across all sites. Notably, the smaller leaves of *Senna siamea* and *Dalbergia sissoo* prevent PM from being resuspended in the air by strong winds, enhancing their overall performance in combating PM pollution. The SEM-EDS analysis was then employed for morphological and chemical characterizations of the PM, revealing anthropogenic sources as the primary contributors to pollution. Hazardous elements, including arsenic (As), antimony (Sb), iron (Fe), indium (In), terbium (Tb), chlorine (Cl), and iodine (I), were identified, underscoring potential health risks associated with the PM composition. The study underscores the significance of SEM-EDS based plant selection for mitigating airborne PM pollution and improving air quality. *Senna siamea* and *Dalbergia sissoo* are identified as top choices for effective PM removal, marking a significant step towards sustainable urban environments. The findings contribute valuable insights into the chemical makeup of PM, facilitating a deeper understanding of its sources and potential health implications. Overall, this research serves as a crucial step in developing strategies to combat air pollution and fosters the creation of healthier and more sustainable urban environments.

Keywords RSPM, SEM-EDS, Image J, Urban Greening, Toxic elements, Heavy metals

In the atmospheric aerosol system, particulate matter (PM) is described as a solid and liquid mixture of organic and inorganic components¹. According to its aerodynamic diameter, it can be divided into total suspended PM (TSPM), PM₁₀ (coarse particles Da ≤ 10 μm), PM_{2.5} (fine PM Da ≤ 2.5 μm), and PM₁ (fine PM Da ≤ 1 μm)^{2,3}. Several studies have indicated that PM₁₀ can enter the respiratory tract of humans and PM_{2.5} can even enter the alveoli region of human lungs. [e.g.,^{4–6}] It causes many severe health issues, including non-fatal heart attacks, impaired lung function, heart problems, breathing problems and coughing, aggravated asthma, and enhanced

¹Department of Botany, Guru Ghasidas Vishwavidyalaya, (A Central University) Koni, Bilaspur, C.G 495009, India. ²Department of Botany, Government Shankar Sao Patel college Waraseoni, Balaghat, MP 481331, India. ³Department of Chemistry, L.B.S. College, Baloda, Janjgir-Champa, C.G 495559, India. ⁴National Taiwan University, Taipei, Taiwan. ⁵Department of Environment, Faculty of Environmental Sciences, King Abdulaziz University, 80203, Jeddah 21589, Saudi Arabia. ⁶Department of Biological Sciences, Faculty of Science, King Abdulaziz University, Jeddah 21589, Saudi Arabia. ⁷Princess Dr Najla Bint Saud Al-Saud Center for Excellence Research in Biotechnology, King Abdulaziz University, Jeddah 21589, Saudi Arabia. ⁸University Centre for Research and Development (UCRD), Chandigarh University, Mohali, Punjab, India. ⁹Department of Botany, Government Naveen College, Kunda, Kabirdham 491559, India. ¹⁰Centre of Excellence in Bionanoscience, King Abdulaziz University, Jeddah, Saudi Arabia. ¹¹Department of Public Health, Daffodil International University, Dhaka 1341, Bangladesh. ✉email: rashmibhu@gmail.com; skpbhu@gmail.com; pandey.sudhir@ggu.ac.in

respiratory symptoms like inflammation of the airways^{7,8}. Additionally, it can harm the brain by entering through the olfactory nerves⁹.

In the present scenario of developing countries, atmospheric PM is a major problem for living beings due to their associated health issues. Particulate matter concentrations are rising daily as a result of fast urban development, industrialization, unplanned growth, construction projects, and a sharp rise in the number of vehicles^{10–12}. For instance, in a recent study in Beijing, China, 78.8% of people were mostly affected by PM_{2.5}, whereas 19.8% were mostly affected by PM₁₀⁶. According to the United States Air Quality Index (US AQI), three Indian cities, Delhi, Kolkata, and Mumbai, are among the most polluted in the world, with Delhi topped the list and listed in the category of “extremely unhealthy cities.” In Bilaspur city of Chhattisgarh, air quality has been deteriorating for a long time due to fast urban development. According to the Central Pollution Control Board (CPCB), the annual permissible limit for PM₁₀ is 60 µg/m³, and for PM_{2.5}, it is 40 µg/m³. The World Health Organization (WHO) also establishes limits for PM concentration in the air, with an annual permissible limit of 20 µg/m³ for PM₁₀ and 10 µg/m³ for PM_{2.5}¹³. In these cities, PM_{2.5} seems to be the main pollutant. The concentration of PM_{2.5} in Bilaspur currently exceeds the WHO annual air quality guideline value by more than 10 times¹⁴ (<https://www.iqair.com/in-en/india/chhattisgarh/bilaspur>). The annual PM concentration for PM₁₀ ranges from 55 to 80 µg/m³, and at times, it has been observed to exceed 150 µg/m³. The annual PM_{2.5} concentration ranges from 40 to 60 µg/m³, with occasional reports of levels reaching up to 140 µg/m³¹⁵.

Despite ongoing efforts, current attempts to reduce environmental pollution have not effectively addressed the causes of contamination. Therefore, there is an urgent need to develop strategies for reducing air pollution. Urban greening is mainly served by plants, which provide many ecosystem services like maintaining ecological balance, temperature control, humidity control, and air purification by fixing the PM^{2,16–18}. Therefore, it is crucial to research how urban vegetation affects atmospheric PM retention and thereby select plants with high retention capacities. The retention ability of PM is different across different plant species, and the retention capacity is an important indicator for the selection of plants for urban greening^{16,19,20}. The retention ability of PM on plant leaf surfaces is affected by environmental factors such as precipitation and temperature. It is also affected by the leaf micromorphological characteristics, including leaf texture, shape, size, roughness, stomatal density, epidermal trichomes, and epidermal waxes^{21–24}.

There are continuous efforts to plant more and more vegetation to control PM pollution. However, there is a lack of a systematic, rapid approach for evaluating plant performance to select the best plant species. To this end, the use of scanning electron microscopy (SEM) with energy-dispersive spectroscopy (EDS) for the morphological and elemental study of PM as well as the selection of suitable plants for their remediation through SEM micrographs, is proposed. In this study, experiments were conducted to select the most suitable plants for the removal of PM from the air in fast-growing urban areas, specifically in Bilaspur, Chhattisgarh, which serves as a representative of such areas. Four sites were chosen for experimentation, employing a meticulous selection process to identify six distinct plant species from these diverse locations. Leaf samples were collected and analyzed using SEM-EDS. Initially, the morphological analysis was conducted using SEM micrographs, and an elemental study was performed using EDS graphs for source identification of PM. Subsequently, SEM micrographs were further analyzed to count PM in different size ranges to determine which plant is better for the accumulation of PM, especially in the respirable range (< 10 µm). Thus, a comprehensive analysis was conducted for PM source identification, as well as the selection of the most suitable plant species for the remediation of airborne PM.

Materials and methods

Study area

Bilaspur, Chhattisgarh, is located in the central part of India. Bilaspur district is situated between 21°47'N to 23°8'N and 81°14'E to 83°15'E. The district of Bilaspur has a subtropical, semiarid, continental, and monsoon climate, and according to Koppen and Geiger²⁵, Bilaspur is in a tropical savanna climate zone. The annual mean temperature ranges between 25 and 27 °C (<https://bilaspur.gov.in/en/>), and the annual precipitation is 1412 mm²⁶. The city is traversed by the national roads Bilaspur-Raipur (NH 130), Bilaspur-Ambikapur (NH 111), and Bilaspur-Raigarh (NH 49). As a result, the air is heavily polluted, such as with PM¹⁶. The study was carried out at four different sites in the Bilaspur city, namely, the 1st site is a roadside of the National Thermal Power Corporation (NTPC) industrial area Bilaspur (IA-1) 20 km from the Bilaspur city. 2nd is the Sirgitti industrial area green belt (IA-2) 8 km from Bilaspur city. 3rd is Bilaspur-Raipur national highway NH 130 roadside (ROS) 6 km from the Bilaspur city, and 4th is Bilaspur-Mungeli national highway (residential/commercial area) NH 130-A residential site (RES) 2 km from the Bilaspur city (Fig. 1; Table 1). These sites were selected because they served as sources of PM pollution, and they were strategically located in different directions within Bilaspur city, allowing us to gain insights into PM pollution levels across various areas of the city.

Plant species selection

The selection of plants for this study was done based on the following factors: (a) The plants should be abundant in the selected areas. (b) Should occur at all the selected sites. (c) The chosen plants should have an ambient height of more than 5 feet for capturing the PM in the respirable zone of humans.

A total of six plant species qualified for the above-mentioned criteria. As such, the selected plants were *Alstonia scholaris* (White Cheesewood), *Dalbergia sissoo* (North Indian rosewood or shisham), *Polyalthia longifolia* (false ashoka), *Millettia pinnata* (Indian Beech), *Senna siamea* (Kassod Tree and Thailand

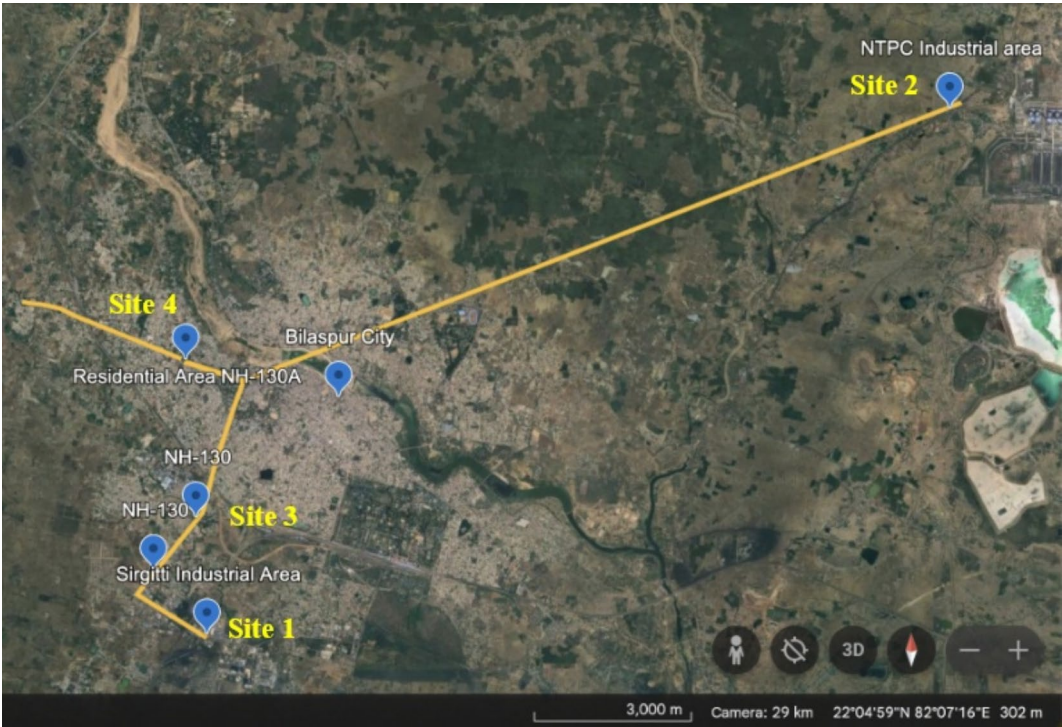


Fig. 1. Location of study sites selected in this study. Image source = Google Earth Version – 10.66.0.1, ©2023. (<https://earth.google.com/web/@22.09352229,82.15720342,287.78127606a,23930.81571272d,35y,0h,0t,0r/data=CgRCAggBOgMKATBCAggASgglhZGY4wEQAA>).

S.N.	Type	Site Information	Description
1	Industrial Area (IA-1)	Site-1 is at around Sirgitti, industrial growth center Sirgitti is situated in Belha Tehsil in Bilaspur district of C.G. (22°02'39.6"N 82°08'11.3"E).	About 338 hectares are covered by this industrial sector. 4431 people are directly employed by 324 industries that have previously been formed with fixed investments totalling more than Rs. 447 crores. 22 km of street lighting with 408 SVLs 8 tube wells, 24 km of pipe, 2 sump wells, and 5 pump houses make up the water delivery infrastructure. 33/11 KV electricity substation is also present.
2	Industrial area (IA-2)	Site-2 is at around a coal-field Thermal Power Plant, NTPC, Sipat, Chhattisgarh. (22°04'40.6"N 82°08'22.8"E).	The Sipat NTPC is one of NTPC's coal-based power facilities. South Eastern Coalfields Limited's Dipika Mines provide the coal used in the power plant. The project, which comprises two phases, has a total installed capacity of 2980 megawatts (MW). Stage one, which was late in getting started, included three units with a combined 660 MW and used super-critical boiler technology. Stage two included two units with a combined 500 MW. The main source of energy in this industry is fossil fuels like Coal, oil, and natural gas. Products formed during combustion of fossils Fuels is PM, CO ₂ , CO, SO ₂ , Volatile Organic Compounds (VOC), Hydrocarbons (HCS), and nitrogen oxides (NO _x) etc.
3	Road side (ROS)	Site-3 is located along national highway (NH130) at Bodri, Bilaspur (C.G.). (22°02'46.4"N 82°07'11.9"E).	NH-130 is a national highway of India. It connects Ambikapur-Katghora-Bilaspur-Raipur. NH-49 and NH 130 A is the junction of NH 130 in Bilaspur. The NH is main source of transportation, and connecting link between different states and industries. Heavy traffic load with transportation of fossil fuels like coal and petroleum is transported.
4	Residential site (RES) Or Commercial mixed area	Site-4 is located near the roadside area at Sanjay Taran Pushkar, Mangla Chowk, Bilaspur Chhattisgarh (22°05'23.7"N 82°07'57.5"E).	The selected site is the centre of the city that covers both commercial and residential areas with heavy traffic load all the day. The site is densely populated, commercial shops load is also cause of the heavy traffic load and pollution.

Table 1. Description of study sites.

Shower), and *Syzygium cumini* (Black plum and jamun). These six plant species are abundantly present in the Bilaspur area, with most of them being native to the region.

Sampling of plant leaves

The sampling of plant leaves took place in May 2022, during the summer season, following 15 days without rain. Leaf samples were collected from the ambient height of 1.5 to 2 m, corresponding to the respirable range, at all selected sites. Leaves were collected from 3 to 5 plants of each selected species for random sampling at every chosen site. The selected leaves were healthy and free of infection to avoid contamination. To ensure uniformity, all samples were collected on the same day, eliminating any potential influence of the sampling date on atmospheric PM retention. Approximately 10–15 mature leaves were gathered from 3 to 4 plants at the specified height of 1.5–2 m, simulating ambient conditions for the study

of PM accumulation. In the 15 days preceding the sampling, the weather conditions at all selected sites were as follows: (a) Wind direction varied, with percentages for different directions such as SE (10.71%), NW (11.60%), SW (10.71%), SSW (16.07%), SSE (12.5%), NE (8.03%), NNW (8.92%), S (8.03%), and all other directions (13.43%). (b) The temperature ranged between 30 and 46 °C. (c) Relative humidity varied from 18 to 43%. (d) No rainfall was recorded (<https://www.worldweatheronline.com/bilaspur-weather/>). Plastic gloves were employed during the sample collection process, and the leaves were precisely cut using scissors. All samples were collected using branches, which were neatly chopped and tightly held to prevent the loss of atmospheric PM from the leaves. Subsequently, the collected leaves were placed in Ziploc bags to mitigate the risk of further contamination and were transported to the laboratory for subsequent analysis.

Morphological and chemical characterization of PM by SEM-EDS

The morphological and elemental composition was assessed through SEM-EDS-based analysis of plant leaves. The leaf was carefully cut into a 1 cm² square piece without disturbing the trapped PM on its surface. Subsequently, the sample underwent a sequential treatment process. It was initially treated with 0.25% glutaraldehyde solution and then transferred to a phosphate buffer solution. After that, samples were treated with a series of concentrations of acetone (20, 40, 60, 80), and stored in 100% acetone. The prepared sample was mounted onto an aluminum stub by double-sided sticky tape, and it was coated with thin conductive film of platinum by ion sputter coater JEOL, Japan (JFC 1600, auto fine coater) and Critical Point Dryer (CPD) Emitech K 850 of Quorum Technology of the UK. These coated samples were analyzed using SEM (JSM 6490) at 15 kV. The micrograph of the leaf sample captured at different magnifications at random points, including 2000x for morphological analysis and 300x and 500x for particle counting at 15 kV and 1280 × 960 resolution. At this resolution in SEM, the particles can be easily distinguished from other substances²⁷. The elemental composition of aggregated particles was resolved using EDS 133, EV Dry Detector (INCA x-act) of OXFORD instruments, UK.

PM counting by Image J

Particle counting was conducted using SEM micrographs analyzed with Image J software, following the methodology described by Ottelé et al. in 2010²⁷. The Image J software analyzes every pixel of the images provided by the SEM. We input the size ranges, and it automatically counts the particles. For this study, SEM micrographs of each leaf sample were captured at random points employing 300x and 500x magnifications at 15 kV resolution for counting particles of all size ranges. SEM micrographs were taken from three randomly selected leaves, chosen from the 10–15 sampled leaves of each plant species. Therefore, triplicate data were obtained from all the selected plants at each site.

To facilitate particle analysis, the images were converted into binary (black and white) format, enabling effective differentiation of PM from the leaf surface, as illustrated in Fig. 2a and b, representing pre- and post-threshold stages. An automatic threshold function was utilized in this study. Some particles appeared overlapped, necessitating the use of the watershed tool within the Image J software to separate these aggregated particles. Once the scale was set, the software automatically quantified the PM on the leaf surface^{27–29}.

Statistical analysis

The statistical analysis was performed using the Statistical Package for the Social Sciences, Version 16 (SPSS-16, IBM, Chicago, USA). To assess the significance of differences in PM counting across all selected plants and sites, an analysis of variance (ANOVA) test was applied, followed by a post hoc multiple comparison with Tukey test. The aim of this analysis was to compare the performance of various plant

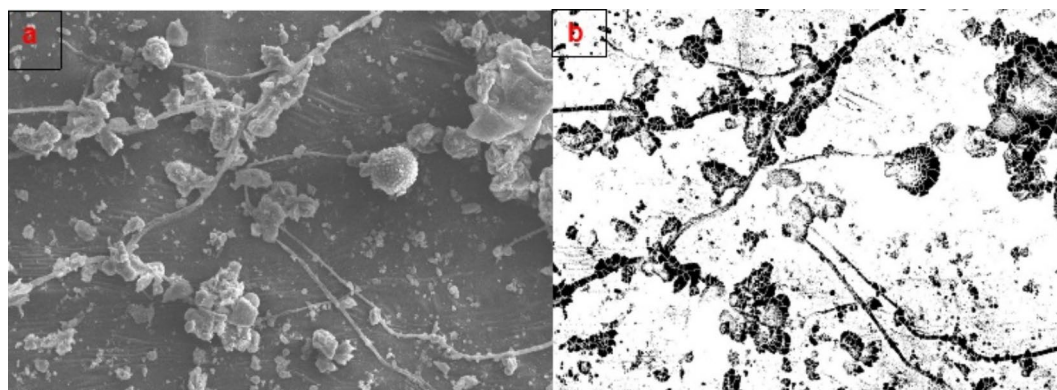


Fig. 2. Analysis of PM at leaf surface through Image J software (a) before threshold and watershed (b) after threshold and watershed.

species across different sites to identify which plants were more effective in the accumulation of PM. The level of significance (p-value) was set at a level of <0.05 . Excel 2021 was used to draw the graph.

Results

Morphological and chemical characterization of PM

The morphological character of PM exhibited diverse shapes, including rounded smooth surfaces, spheroidal and spherical particles with rough surfaces, large irregular shapes, large crystal shapes with sharp ends, amorphous or irregular shapes, irregular flat shapes, agglomerate and free shapes, aggregate spherical particles, sharp-ended particles, and ovoid types. These characteristics were evident in SEM images of leaf surfaces (Fig. 3). The probable sources of PM, determined by their morphological characteristics, are described in Table S1.

Additionally, the elemental composition of the PM was determined through EDS spectra, revealing a complex mixture of components, such as aluminum (Al), antimony (Sb), arsenic (As), calcium (Ca), carbon (C), chlorine (Cl), indium (In), iodine (I), iron (Fe), magnesium (Mg), oxygen (O), potassium (K), silicon (Si), sodium (Na), sulphur (S), terbium (Tb), titanium (Ti), and zirconium (Zr). The combination of PM composition and distinct morphological features provides a potential means to identify the sources of PM in the environment³⁰.

At site 1 (IA-1), the PM compositions by EDS spectra include Al, C, Ca, Fe, In, K, Mg, Na, O, S, Si, Ti, and Zr. At site 2 (IA-2), the composition consists of Al, C, Ca, Fe, I, In, K, Mg, Na, O, S, Sb, Si, Tb, and Ti. At site 3 (ROS), PM consists of Al, As, C, Ca, Fe, K, Mg, O, S, Sb, Si, and Zr elements. Site 4 (RES) PM consists of Al, C, Ca, Cl, Fe, I, In, K, Mg, Na, O, S, Si, and Zr. According to EDS spectra, the compositions reveal that the PM comes from both anthropogenic and natural sources.

PM counting by image j

The amount of PM in different size ranges was found to be in the order of $IA-1 > IA-2 > ROS > RES$ for most of the plants (see Figs. 4 and 5, and 6). In the case of PM in the 10–100 μm (non-respirable) range, four sites were considered. At IA-1, *Polyalthia longifolia* and *Dalbergia sissoo* showed a significantly higher PM count compared to the other four plants ($P < 0.05$). IA-2 had less PM in the non-respirable range compared to other sites. IA-2, being a thermal power industrial zone, mainly emits PM in the respirable range. In IA-2, *Syzygium cumini* showed the highest PM accumulation compared to all other plants. The ROS site had more PM in this range compared to other sites, and *Polyalthia longifolia* and *Dalbergia sissoo* showed a significantly higher PM count than other plants ($P < 0.05$). RES is a residential site, which is why the PM count is lower compared to ROS and IA-1. In this site, *Dalbergia sissoo* and *Alstonia scholaris* showed better performance than other plants.

In the non-respirable range, we didn't observe a clear pattern indicating which plant is best for PM removal in this range. However, *Polyalthia longifolia* and *Dalbergia sissoo* showed higher PM counts at three sites (IA-1, ROS, and RES) (Fig. 4). *Polyalthia longifolia* has large leaves, large trichomes, unique foliar arrangements, a fibrous midrib, and a waxy coating on the leaf surface, all of which help in the retention of larger-sized PM³¹. *Dalbergia sissoo* also performed well in three different sites (IA-1, ROS, and RES). This is likely due to the roughness of the leaves and their unique morphology^{16,32}.

PM of size less than 10 μm falls under the criteria of the respirable PM range, which is mostly harmful for humans. In the range of PM_{10} (2.5–10 μm), *Dalbergia sissoo* and *Senna siamea* showed significantly higher accumulation at all four sites ($P < 0.05$) (Fig. 5). At site IA-1, *Dalbergia sissoo* and *Senna siamea* displayed the highest PM count ($P < 0.05$). At site IA-2, only *Senna siamea* showed a significantly higher PM count compared to all other five plants ($P < 0.05$). At site ROS, *Dalbergia sissoo* showed a significantly higher PM count ($P < 0.05$) compared to other plants, and *Senna siamea* also performed well at this site (Fig. 5). At the RES site, both *Dalbergia sissoo* and *Senna siamea* exhibited a significantly higher PM count compared to all other four plants ($P < 0.05$). Overall, *Dalbergia sissoo* and *Senna siamea* showed better performance in PM remediation within the PM_{10} range.

Discussion

Morphological and chemical characterization of PM

It was observed that smooth surface PM was found in large amounts in both industrial areas (IA-1 and IA-2). This indicates that smooth surface particles are mostly associated with industrial areas. PM of rough surface were found present in all areas. However in the residential area (RES), the number of such particles was significantly higher. The reason behind this could be the resuspension of soil particles due to heavy vehicular activities.

At IA-1, PM consists of elements such as Al, Ca, Fe, K, Mg, O, Si, Ti, and Zr, which are naturally abundant in soil and the earth's crust^{33–35}. They often accumulate on leaves due to air pollution from heavy vehicles in industrial areas^{36,37}. Major sources of Fe dust include railways and iron and steel industries, which can lead to health issues when mixed with oxygen, forming iron oxides and causing conditions like metal fume fever, abdominal pain, vomiting, and constipation³⁸. Carbon emissions originate from coal combustion and coal-based industries, causing respiratory problems and the formation of carbon monoxide (CO), leading to symptoms like headaches and dizziness³⁹. Potassium and Na emissions are associated with steelworks, coal burning, and incinerators^{40,41}. Sulfur can result from fossil fuel burning by power plants and motor vehicles, causing irritation to the skin and mucous membranes⁴². Indium is released from the electronics, photovoltaics, and LED industries, and its compounds can lead to health issues such as lung cancer and interstitial pneumonia^{43,44}. Site 1 is the central hub of industries in Bilaspur city, and these industries release harmful substances into the air, creating pollution and potential health risks. These elements are present in the air at this site and may be transported by the wind.

IA-2 contains the rare earth metal Tb, not found at any other sites³³. Terbium is released from mining activities and can be irritating to the skin and eyes³³. Additionally, IA-2 has a high carbon content due to NTPC, a major coal-based thermal power company, generating carbon particles from coal fuel. This results in

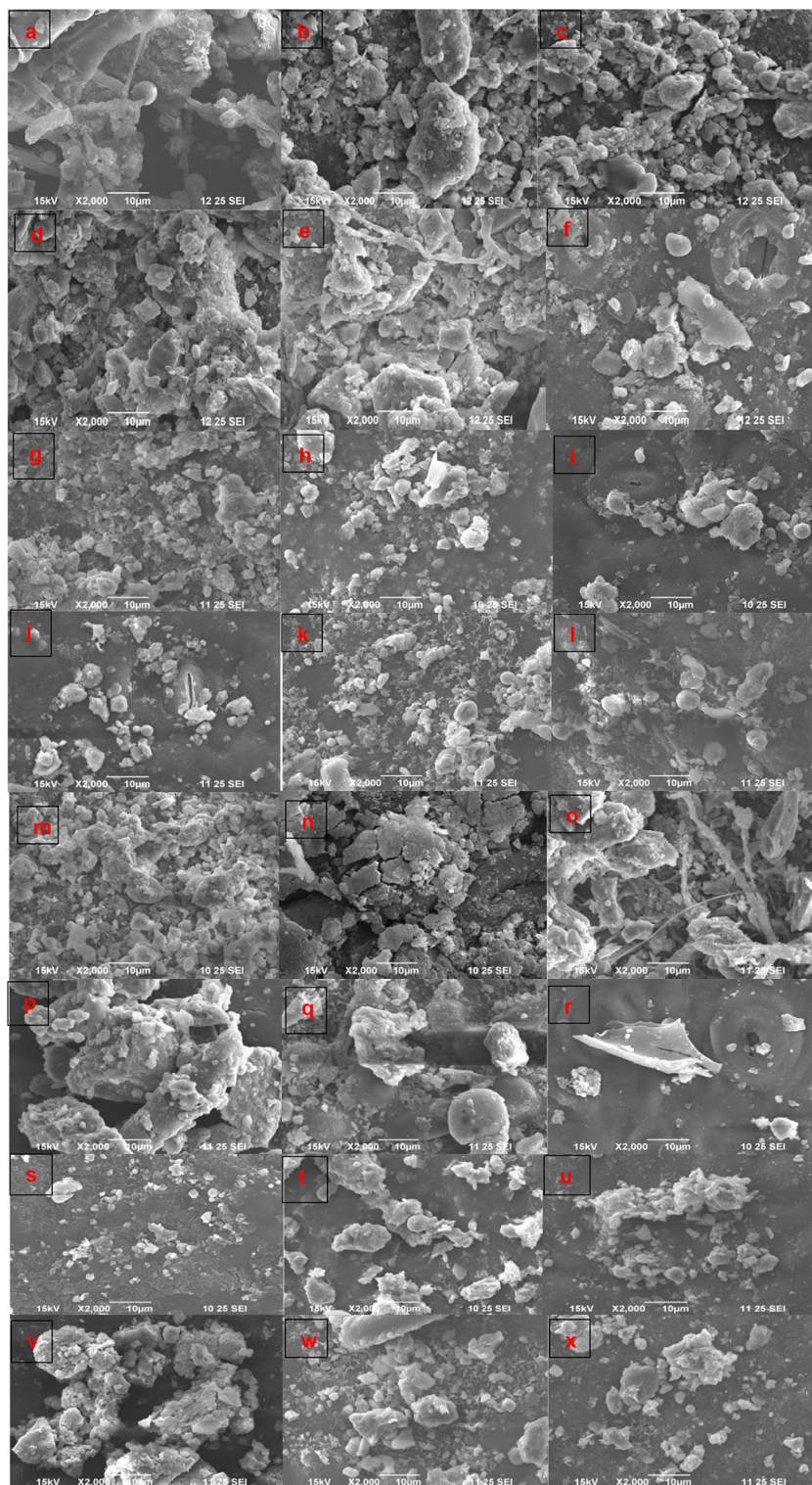


Fig. 3. Morphological differences of PM present at the leaf surfaces of selected (six) plant species at all four sites a–f from site 1 (IA-1), g–l from site 2 (IA-2), m–r from site 3 (ROS), s–x from site 4 (RES). All SEM micrograph are in a series of *Alstonia scholaris*, *Dalbergia sissoo*, *Polyaltha longifolia*, *Millettia pinnata*, *Senna siamea*, and *Syzygium cumini*.

a higher carbon percentage compared to other elements. Terbium may also be associated with heavy vehicles that directly come from mining sites, contributing to its additional presence in the air. ROS shares common elements with IA-1, including Al, Ca, Fe, K, Mg, O, and Si. Additionally, ROS has As and Sb. The source of As is coal burning, burning vegetation, and coal-based industries^{45–47}. A recent study showed that As is also

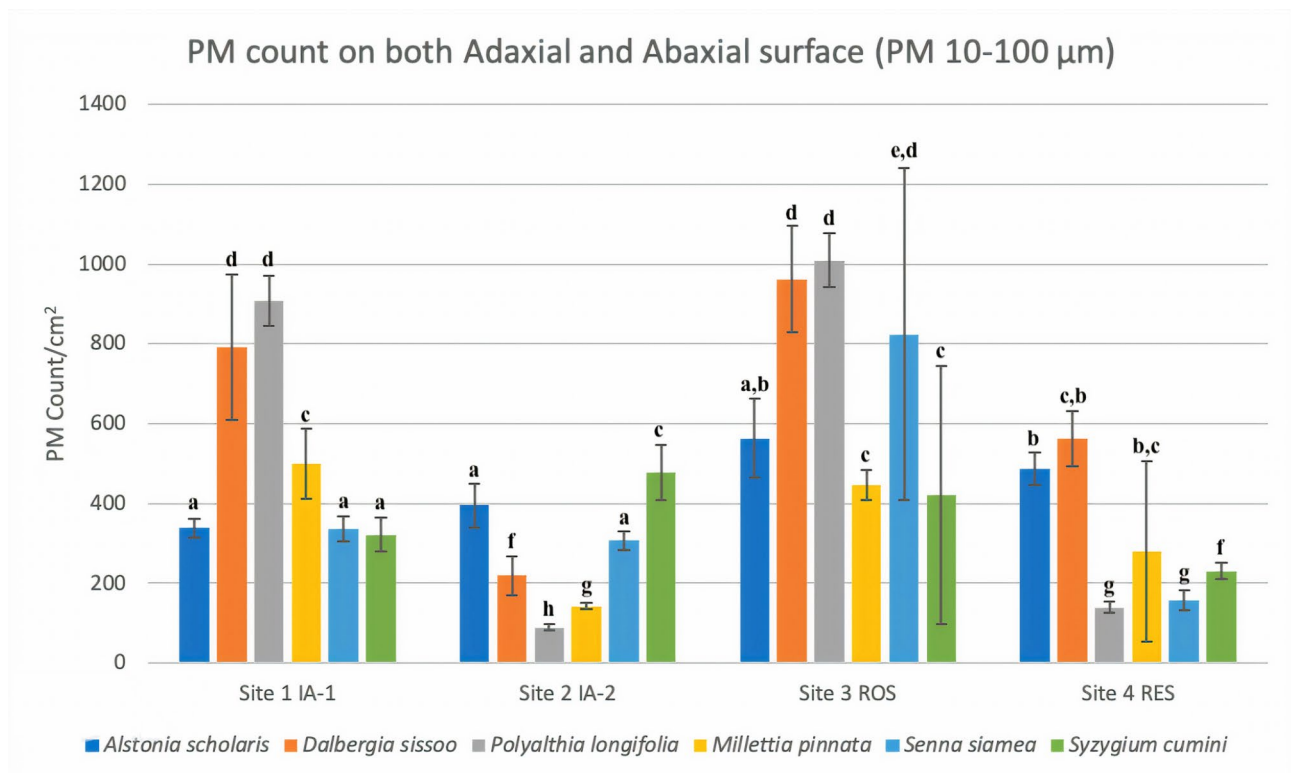


Fig. 4. Number of PM particles in 10–100 μm (non-respirable range) across selected plant sp. at four different study sites. Different alphabets shows significant variation ($P < 0.05$) and same alphabets shows homogeneity ($n = 3$).

emitted from the pharmaceutical and cosmetic industries⁴⁸. According to the International Agency for Research on Cancer (IARC), As is a very toxic and carcinogenic metalloid⁴⁹. Arsenic can cause health issues, including cancer, skin lesions, cardiovascular disease, and diabetes. Arsenic exposure may also produce free radicals and alter the methylation status of cellular DNA, leading to a significant impact on liver cells^{50–52}. Particulate matter can absorb large quantities of As, increasing the risk of exposure through inhalation and ingestion^{51,52}. The majority of Sb emissions come from high-temperature combustion operations, and as a result, they are emitted as submicron particles that can rapidly aggregate in a bulk mode, as indicated by $\text{PM}_{2.5}$ ^{53–55}. Additionally, waste from the cosmetics and pharmaceutical sectors releases Sb^{48,56}. Antimony and its compounds are very harmful to human health and can even be carcinogenic⁵⁷. The United States Environmental Protection Agency (USEPA) considers Sb and related compounds to be priority pollutants⁵⁸. Long-term industrial exposure can cause respiratory irritation and, in some cases, lead to pneumoconiosis with obstructive lung changes in humans. It can also harm the eyes, lungs, heart, and skin⁵⁹. High C content is attributed to the proximity to Sirgitti and the transport of C by air, along with heavy coal vehicle traffic from IA-1.

RES shares similarities with IA-1 and ROS but includes additional elements, Cl and I. Chlorine comes from cooling towers, swimming pools, and water purification facilities in residential area⁶⁰. Chlorine, when combined with soil dust, can cause respiratory illness, asthma, chest pain, vomiting, changes in breathing, and cough⁶¹. Iodine is emitted from restaurants and street food stalls because they use different types of salt for making foods.

PM counting by image j

Particulate matter size less than 2.5 μm , also known as fine particles, was counted using the Image J technique. In the range of $\text{PM}_{2.5}$ (0.2–2.5 μm), *Dalbergia sissoo* and *Senna siamea* showed significantly higher accumulation at all four sites ($P < 0.05$) (Fig. 6). At IA-1, the highest PM count was retained by *Senna siamea* and *Dalbergia sissoo* compared to *Polyalthia longifolia* ($P < 0.05$). *Senna siamea* and *Dalbergia sissoo* also showed the highest PM count at site IA-2 (Fig. 6). At ROS, *Dalbergia sissoo* showed a significantly higher PM count compared to other plants, and *Senna siamea* also performed well at this site. Since RES is a residential site, the PM concentration is lower compared to other sites, and *Senna siamea* significantly showed the highest PM count at this site ($P < 0.05$) (Fig. 6). One recent study by Gajbhiye et al.⁶² compared two different plants by using SEM-EDS based rapid method, and identified *Senna siamea* is more suitable for the urban greening program.

In the respirable range of PM_{10} and $\text{PM}_{2.5}$, *Senna siamea* and *Dalbergia sissoo* were found to be the best plants for PM retention. These plants are evergreen, so leaves are always present on the plants. *Dalbergia sissoo* has unique surface morphology¹⁶. This plant has small leaves that prevent wind force, which is responsible for PM resuspension in air. Its leaves have special characteristics such as a rough surface, small pits and grooves on the surface, and small trichomes^{16,63}. Anisocytic type of stomata is present in this plant, and the stomatal density is

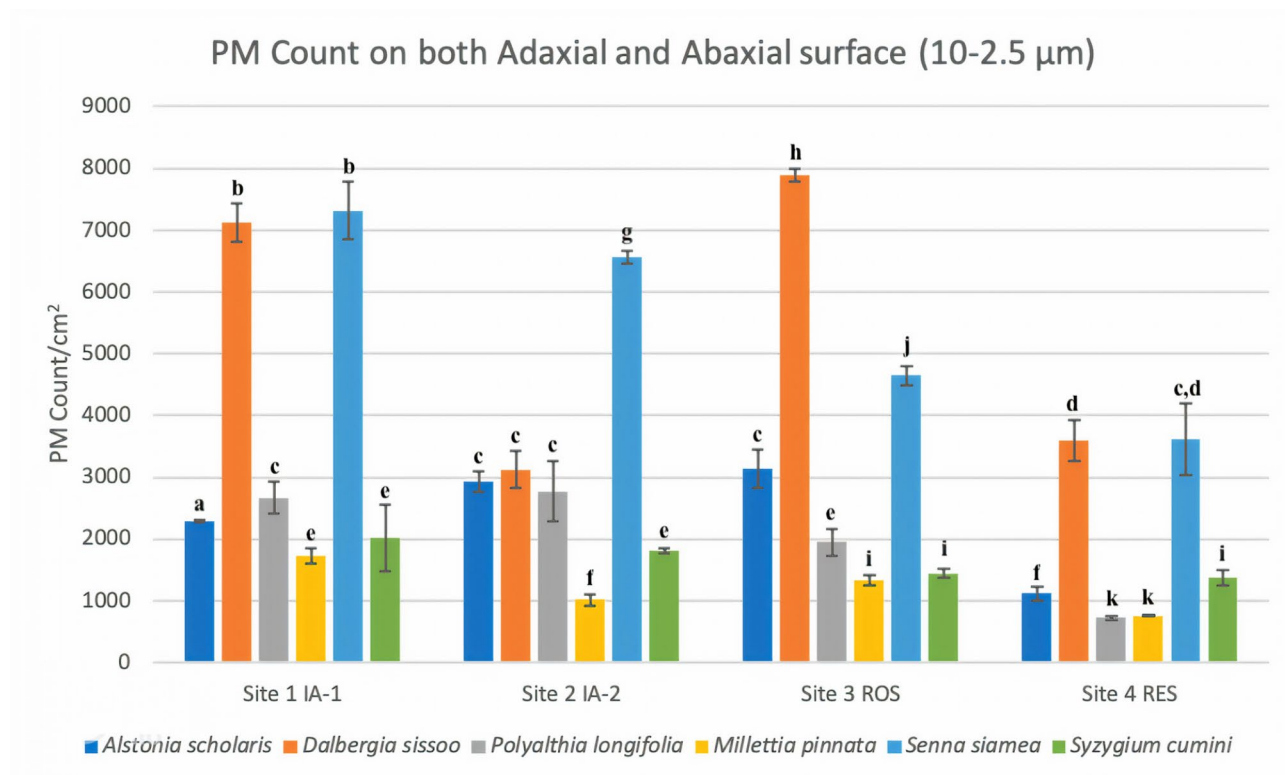


Fig. 5. Number of PM particles in 10–2.5 µm coarse (respirable range) across selected plant sp. at four different study sites. Different alphabets shows significant variation ($P < 0.05$) and same alphabets shows homogeneity ($n = 3$).

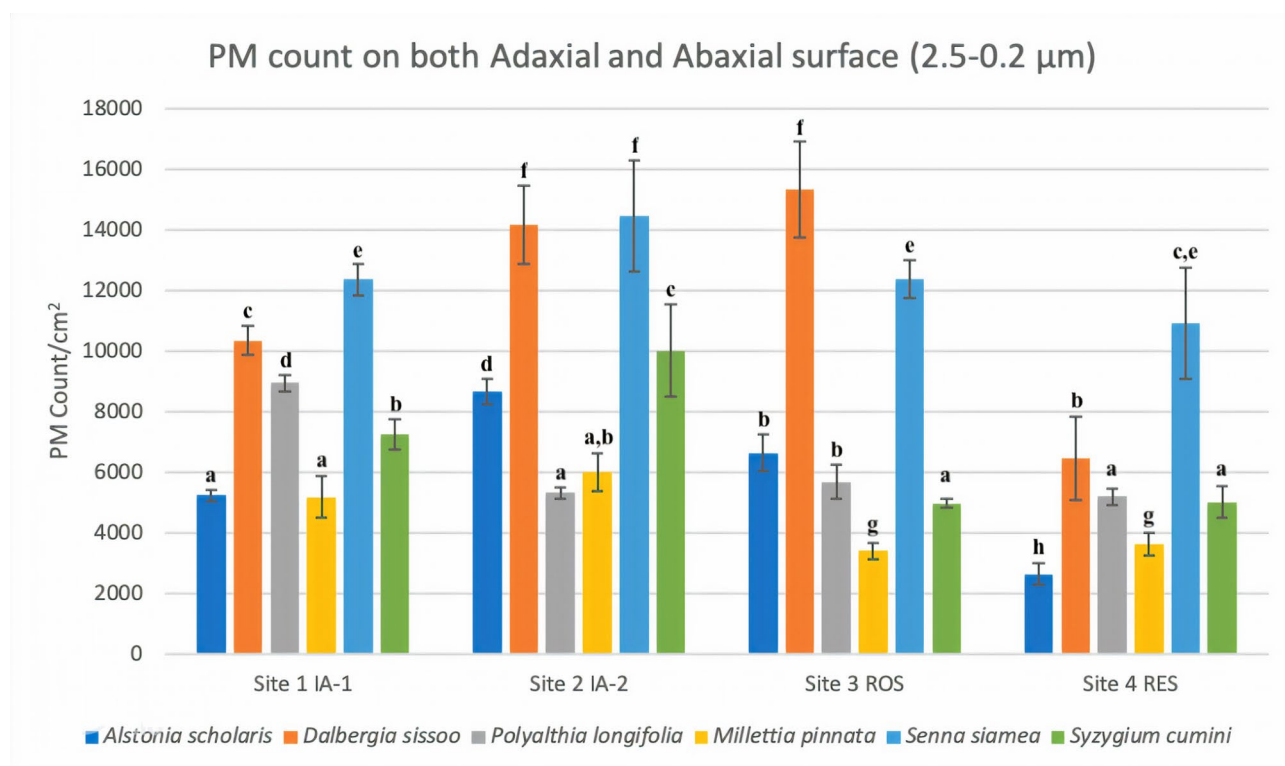


Fig. 6. Number of PM particles in 0.2–2.5 µm (respirable range) across selected plant sp. at four different study sites. Different alphabets shows significant variation ($P < 0.05$) and same alphabets shows homogeneity ($n = 3$).

S.N.	Plant name	Family	Leaf Shape	Epicuticular wax		Stomata		Trichome	
				Adaxial	Abaxial	Adaxial	Abaxial	Adaxial	Abaxial
1	<i>Alstonia scholaris</i>	Apocynaceae	elliptic-oblancoate	+	+	-	+	+	+
2	<i>Dalbergia sissoo</i>	Fabaceae	broad ovate	-	+	+	+	+	+
3	<i>Polyalthia longifolia</i>	Annonaceae	narrow or linier lanceolate	+	+	+	+	-	+
4	<i>Millettia pinnata</i>	Fabaceae	ovate	+	+	-	+	-	+
4	<i>Senna siamea</i>	Fabaceae	ovate	+	+	+	+	+	+
6	<i>Syzygium cumini</i>	Myrtaceae	elliptic to broadly oblong	-	-	-	+	+	-

Table 2. Selected plant species with their unique leaves' morphological features.

also high⁶⁴. All these characteristics contribute to the accumulation of a large amount of PM. *Senna siamea* is the best-performing plant in the respirable PM range. This plant has a group of small leaves (compound leaves). The leaf surface has unique characteristics such as a rough surface and smaller rough trichomes, which are responsible for accumulating a large amount of PM^{24,62}. The stomata are also responsible for PM accumulation in *Senna siamea*; it has three different types of stomata, such as polygonal, aniscocytic, and paracytic, present on the adaxial and abaxial sides. The rough surface of trichomes is very helpful for the retention of PM in the respirable range^{62,65}. *Dalbergia sissoo* and *Senna siamea* are the best plants for retaining airborne particulate matter (PM) compared to other selected species. This is primarily due to their unique morphological characteristics; in these two plants, stomata and trichomes are present on both the adaxial and abaxial surfaces of their leaves (Table 2), which distinguishes them from other plants. This unique feature enables them to perform exceptionally well, particularly in retaining PM in the respirable range. One recent study compared different methodologies for PM quantification accumulated on leaves and microscopy-based method was found best as compare to other quantification methods such as gravitational and sensor based^{16,66}.

Conclusion

The research concludes that the SEM-EDS-based method is a quick approach for the comprehensive investigation of airborne PM, including their source identification with morphological and elemental composition analysis. The study explored the morphology and chemical composition of PM, identifying anthropogenic sources as significant contributors. Certain elements, such as As, Sb, Fe, C, In, Tb, Cl, and I, were highlighted as posing health risks to humans. The present investigation further revealed that leaf arrangement and morphological characteristics significantly influence PM accumulation, with *Senna siamea* and *Dalbergia sissoo* exhibiting superior PM retention in both coarse and fine PM ranges. The micromorphological features of these plants, including trichomes, stomatal density, rough surfaces, and leaf shapes, contribute to their effectiveness in PM retention and air purification. Notably, the smaller leaves of *Senna siamea* and *Dalbergia sissoo* prevent PM from being resuspended in the air by strong winds, enhancing their overall performance in combating PM pollution.

Based on the results of this study, *Senna siamea* and *Dalbergia sissoo* were found to be the most effective plant species for mitigating PM pollution. This study demonstrate the efficacy of the employed methods for PM characterization, source identification, and the selection of suitable plant species for urban greening, with a particular focus on PM pollution remediation. As such, this work proposes a strategy for the removal of airborne PM by utilizing green vegetation, providing a natural solution to mitigate air pollution. The key contribution is the identification of suitable plant species for efficiently removing PM from the air, which enhances the effectiveness of green remediation strategies and urban greening. However, the current approach cannot provide the accurate concentration of elements and only indicates their relative proportion. Although the presence of such harmful elements in the air can pose risks to living beings, knowing the actual concentration of these elements is essential to assessing their potential harm to human health. Cross-validation of the procedure adopted in this study with other approaches should offer valuable insights into the characterization of PM. In addition, research should be directed to add specific methods and results of exposure concentration and possible health implications to strengthen the relevance to public health discussions and policy-making.

Data availability

Data will be made available on request to the corresponding author (Dr. S.K. Pandey, skpbhu@gmail.com; pandey.sudhir@ggu.ac.in).

Received: 20 September 2024; Accepted: 24 December 2024

Published online: 17 January 2025

References

- Wu, H. et al. Effects of green space landscape patterns on particulate matter in Zhejiang Province, China. *Atmos. Pollut. Res.* **9**, 923–933. <https://doi.org/10.1016/j.apr.2018.03.004> (2018).
- Muhammad, S., Wuyts, K. & Samson, R. Immobilized atmospheric particulate matter on leaves of 96 urban plant species. *Environ. Sci. Pollut. Res.* **27**, 36920–36938. <https://doi.org/10.1007/s11356-020-09246-6> (2020).
- Xie, Y., Zhao, M., He, J., Chen, Z. & Zhao, J. Dust-retention ability of *Picea Wilsonii* and *Pinus Tabulformis* forest with different diameter classes. *J. Northeast Univ.* **35** (6), 17–24 (2020).

4. Chen, L., Liu, C., Zhang, L., Zou, R. & Zhiqiang, Z. Variation in tree species ability to capture and retain airborne fine particulate matter (PM_{2.5}). *Sci. Rep.* **7**, 3206. <https://doi.org/10.1038/s41598-017-03360-1> (2017).
5. Chen, H. et al. Magnetic characteristics of Juniperus formosana needles along an urban street in Lanzhou, Northwest China: The variation of different season and orientation. *Environ. Sci. Pollut. Res.* **26**, 21964–21971. <https://doi.org/10.1007/s11356-019-0539-9> (2019).
6. Yin, Z., Zhang, Y. & Ma, K. Airborne particulate matter distribution in urban green space is size-dependent. *Urban Urban Green.* **63**, 127196. <https://doi.org/10.1016/j.ufug.2021.127196> (2021).
7. Correia, A. W. et al. The effect of air pollution control on life expectancy in the United States: An analysis of 545 US counties for the period 2000 to 2007. *Epidemiol. (Cambridge Mass.)* **24** (1), 23. <https://doi.org/10.1097/EDE.0b013e3182770237> (2013).
8. Cadelis, G., Tourres, R. & Molinie, J. Short-term effects of the particulate pollutants contained in Saharan dust on the visits of children to the emergency department due to asthmatic conditions in Guadeloupe (French Archipelago of the Caribbean). *PloS One.* **9** (3), e91136. <https://doi.org/10.1371/journal.pone.0091136> (2014).
9. Solomon, P. A. et al. Macroscopic to microscopic scales of particle dosimetry: From source to fate in the body. *Air Qual. Atmos.* **5** (2), 169–187. <https://doi.org/10.1007/s11869-011-0167-y> (2012).
10. Cohen, A. J. et al. Estimates and 25-year trends of the global burden of disease attributable to ambient air pollution: An analysis of data from the global burden of diseases study 2015. *Lancet* **389**, 1907–1918. [https://doi.org/10.1016/S0140-6736\(17\)30505-6](https://doi.org/10.1016/S0140-6736(17)30505-6) (2017).
11. Conibear, L., Butt, E. W., Knote, C., Arnold, S. R. & Spracklen, D. V. Residential energy use emissions dominate health impacts from exposure to ambient particulate matter in India. *Nat. Commun.* **9**, 617. <https://doi.org/10.1038/s41467-018-02986-7> (2018).
12. Lu, S. et al. Effects of plant leaf surface and different pollution levels on PM_{2.5} adsorption capacity. *Urban Urban Green.* **34**, 64–70. <https://doi.org/10.1016/j.ufug.2018.05.006> (2018).
13. WHO. Air quality guidelines. (2023). <https://www.who.int/news-room/feature-stories/detail/what-are-the-who-air-quality-guidelines>
14. IQAir. Air quality of Bilaspur Chhattisgarh. (2022). <https://www.iqair.com/in-en/india/chhattisgarh/bilaspur>
15. Bilaspur, A. Q. I. Bilaspur air quality index. (2022). <https://www.aqi.in/in/dashboard/india/chhattisgarh/bilaspur/>
16. Tiwari, A. et al. A practical option for the selection of suitable plants for the management of airborne particulate matter (PM). *Int. J. Environ. Sci. Technol.* **20** (10), 11537–11548. <https://doi.org/10.1007/s13762-022-04579-w> (2023).
17. Jiang, B. et al. Differences in airborne particulate matter concentration in urban green spaces with different spatial structures in Xi'an. *China Forests.* **13** 14. <https://doi.org/10.3390/f13010014> (2021).
18. Pandey, M. et al. The environmental significance of contaminants of concern in the soil–vegetable interface: Sources, accumulation, health risks, and mitigation through biochar. *Sustainability* **14**, 14539. <https://doi.org/10.3390/su142114539> (2022).
19. Letter, C. & Jäger, G. Simulating the potential of trees to reduce particulate matter pollution in urban areas throughout the year. *Environ. Dev. Sustain.* **22**, 4311–4321. <https://doi.org/10.1007/s10668-019-00385-6> (2019).
20. Lu, T., Lin, X., Chen, J., Huang, D. & Li, M. Atmospheric particle retention capacity and photosynthetic responses of three common greening plant species under different pollution levels in Hangzhou. *Glob. Ecol. Conserv.* **20**, e00783. <https://doi.org/10.1016/j.gecco.2019.e00783> (2019).
21. Sharma, P. et al. Seasonal dynamics of particulate matter pollution and its dispersion in the city of Delhi, India. *Meteor. Atmos. Phys.* **134** (28). <https://doi.org/10.1007/s00703-021-00852-8> (2022).
22. Weerakkody, U., Dover, J. W., Mitchell, P. & Reiling, K. Evaluating the impact of individual leaf traits on atmospheric particulate matter accumulation using natural and synthetic leaves. *Urban Urban Green.* **30**, 98–107. <https://doi.org/10.1016/j.ufug.2018.01.001> (2018).
23. Zhang, X. et al. Effects of the leaf functional traits of coniferous and broadleaved trees in subtropical monsoon regions on PM_{2.5} dry deposition velocities. *Environ. Pollut.* **265**, 114845. <https://doi.org/10.1016/j.envpol.2020.114845> (2020).
24. Gajbhiye, T., Pandey, S. K., Kim, K. H., Szulejko, J. E. & Prasad, S. Airborne foliar transfer of PM bound heavy metals in Cassia siamea: A less common route of heavy metal accumulation. *Sci. Total Environ.* **573**, 123–130. <https://doi.org/10.1016/j.scitotenv.2016.08.099> (2016).
25. Koppen, W. & Geiger, R. Climate classification. (2006). <https://geographyandyou.com/koppen-climate-classification-system/>
26. Climate data. Climate data of Bilaspur. (2023). <https://en.climate-data.org/asia/india/chhattisgarh/bilaspur-2823/>
27. Ottelé, M., van Bohemen, H. D. & Fraaij, A. L. Quantifying the deposition of particulate matter on climber vegetation on living walls. *Ecol. Eng.* **36** (2):154–162. <https://doi.org/10.1016/j.ecoleng.2009.02.007> (2010).
28. Schneider, C. A., Rasband, W. S. & Eliceiri, K. W. NIH Image to ImageJ: 25 years of image analysis. *Nat. Methods.* **9** (7), 671–675. <https://doi.org/10.1038/nmeth.2089> (2012).
29. Tiwari, A., Pandey, M., Tirkey, A., Pandey, S. K. & Kim, K. H. Methods for the analysis of airborne particulate matter. *Interdiscip. Environ. Rev.* **22** (1), 18–42. <https://doi.org/10.1504/IER.2022.122999> (2022).
30. Tiwari, A. et al. Image based analytical approaches for study of particulate matter (PM) in air. *Front. Environ. Sci.* **12**, 1362422. <https://doi.org/10.3389/fenvs.2024.1362422> (2024).
31. Shenoy Heckadka, S., Nayak, S. Y., Kamath, C. R., Adarsh, S. P. & Samant, R. Characterization of a novel polyalthia longifolia mid-rib fibers as a potential reinforcement for polymer composites. *J. Nat. Fibers.* **19** (6), 2106–2118. <https://doi.org/10.1080/15440478.2020.1798847> (2022).
32. Mo, L., Ma, Z., Xu, Y., Sun, F., Lun, X., Liu, X. & Yu, X. Assessing the capacity of plant species to accumulate particulate matter in Beijing, China. *PloS One.* **10** (10), e0140664. <https://doi.org/10.1371/journal.pone.0140664> (2015).
33. Genga, A., Baglivi, F., Siciliano, M., Siciliano, T., Tepore, M., Micocci, G. & Aiello, D. SEM-EDS investigation on PM₁₀ data collected in Central Italy: Principal component analysis and hierarchical cluster analysis. *Chem. Cent. J.* **6** (2), 1–15. <https://doi.org/10.1186/1752-153X-6-S2-S3> (2012).
34. Cong, Z., Kang, S., Dong, S. & Zhang, Y. Individual particle analysis of atmospheric aerosols at Nam Co Tibetan Plateau. *Aerosol Air Qual. Res.* **9** (3), 323–331. <https://doi.org/10.4209/aaqr.2008.12.0064> (2009).
35. Chow, J. C., Watson, J. G., Lowenthal, D. H. & Countess, R. J. Sources and chemistry of PM₁₀ aerosol in Santa Barbara County, CA. *Atmos. Environ.* **30** (9), 1489–1499. [https://doi.org/10.1016/1352-2310\(95\)00363-0](https://doi.org/10.1016/1352-2310(95)00363-0) (1996).
36. Matzka, J. & Maher, B. A. Magnetic biomonitoring of roadside tree leaves: Identification of spatial and temporal variations in vehicle-derived particulates. *Atmos. Environ.* **33** (28), 4565–4569. [https://doi.org/10.1016/S1352-2310\(99\)00229-0](https://doi.org/10.1016/S1352-2310(99)00229-0) (1999).
37. Tiwari, S. et al. Phytomonitoring of hazardous metals in air. *Interdiscip. Environ. Rev.* **22** (3–4), 232–256. <https://doi.org/10.1504/IER.2022.128143> (2022).
38. Jia, J., Cheng, S., Yao, S., Xu, T., Zhang, T., Ma, Y. & Duan, W. Emission characteristics and chemical components of size-segregated particulate matter in iron and steel industry. *Atmos. Environ.* **182** 115–127. <https://doi.org/10.1016/j.atmosenv.2018.03.051> (2018).
39. Rohr, A. & McDonald, J. Health effects of carbon-containing particulate matter: focus on sources and recent research program results. *Crit. Rev. Toxicol.* **46** (2), 97–137. <https://doi.org/10.3109/10408444.2015.1107024> (2016).
40. Taiwo, A. M., Harrison, R. M. & Shi, Z. A review of receptor modelling of industrially emitted particulate matter. *Atmos. Environ.* **97**, 109–120. <https://doi.org/10.1016/j.atmosenv.2014.07.051> (2014).
41. Ooki, A., Uematsu, M., Miura, K. & Nakae, S. Sources of sodium in atmospheric fine particles. *Atmos. Environ.* **36** (27), 4367–4374. [https://doi.org/10.1016/S1352-2310\(02\)00341-2](https://doi.org/10.1016/S1352-2310(02)00341-2) (2002).
42. Begum, B. A., Hopke, P. K. & Markwitz, A. Air pollution by fine particulate matter in Bangladesh. *Atmos. Pollut. Res.* **4** (1), 75–86. <https://doi.org/10.5094/APR.2013.008> (2013).

43. White, S. J. O. & Hemond, H. F. The anthropogeoechemical cycle of indium: A review of the natural and anthropogenic cycling of indium in the environment. *Crit. Rev. Environ. Sci. Technol.* **42** (2), 155–186. <https://doi.org/10.1080/10643389.2010.498755> (2012).
44. Schwarz-Schampera, U. & Indium *Crit. Met. Handb.*, 204–229 <https://doi.org/10.1002/9781118755341.ch9> (2014).
45. Sanchez-Rodas, D., De, L., Campa, A. S., Oliveira, V. & De, L. A. Rosa, J. Health implications of the distribution of arsenic species in airborne particulate matter. *J. Inorg. Biochem.* **108**, 112–114. <https://doi.org/10.1016/j.jinorgbio.2011.11.023> (2012).
46. Wang, J. et al. Bioaccessibility, sources and health risk assessment of trace metals in urban park dust in Nanjing, Southeast China. *Ecotoxicol. Environ. Saf.* **128**, 161–170. <https://doi.org/10.1016/j.ecoenv.2016.02.020> (2016).
47. Tan, J. et al. Chemical characteristics and source apportionment of PM_{2.5} in Lanzhou, China. *Sci. Total Environ.* **601**, 1743–1752. <https://doi.org/10.1016/j.scitotenv.2017.06.050> (2017).
48. Muritala, K. B. & Adewole, J. K. Technical challenges in pharmaceuticals and cosmetics industries in Nigeria: A review of the roles of membrane technology. *Int. J. Membrane Sci. Technol.* **9**(1) (2019).
49. Liu, J. & Waalkes, M. P. Liver is a target of arsenic carcinogenesis. *Toxicol. Sci.* **105** (1), 24–32. <https://doi.org/10.1093/toxsci/kfn120> (2008).
50. Pandey, M., Tirkey, A., Tiwari, A., Pandey, S. K. & Khan, M. L. Microbial interaction of biochar and its application in soil, water and air. In *Microbes and Microbial Biotechnology for Green Remediation* 185–203. <https://doi.org/10.1016/B978-0-323-90452-0.00001-3> (Elsevier, 2022).
51. Minatel, B. C. et al. Environmental arsenic exposure: From genetic susceptibility to pathogenesis. *Environ. Int.* **112**, 183–197. <https://doi.org/10.1016/j.envint.2017.12.017> (2018).
52. Xie, J. J. et al. Fraction distribution of arsenic in different-sized atmospheric particulate matters. *Environ. Sci. Pollut. Res.* **26**, 30826–30835. <https://doi.org/10.1007/s11356-019-06176-w> (2019).
53. He, M., Wang, X., Wu, F. & Fu, Z. Antimony pollution in China. *Sci. Total Environ.* **421**, 41–50. <https://doi.org/10.1016/j.scitotenv.2011.06.009> (2012).
54. Wilson, S. C., Lockwood, P. V., Ashley, P. M. & Tighe, M. The chemistry and behaviour of antimony in the soil environment with comparisons to arsenic: A critical review. *Environ. Pollut.* **158** (5), 1169–1181. <https://doi.org/10.1016/j.envpol.2009.10.045> (2010).
55. Shotyk, W., Krachler, M. & Chen, B. Antimony in recent, ombrotrophic peat from Switzerland and Scotland: Comparison with natural background values (5,320 to 8,020 14 C yr BP) and implications for the global atmospheric Sb cycle. *Global Biogeochem. Cycles*. **18** (1). <https://doi.org/10.1029/2003GB002113> (2004).
56. Bocca, B., Pino, A., Alimonti, A. & Forte, G. Toxic metals contained in cosmetics: A status report. *Regul. Toxicol. Pharmacol.* **68** (3), 447–467. <https://doi.org/10.1016/j.yrtph.2014.02.003> (2014).
57. Hammel, W., Debus, R. & Steubing, L. Mobility of antimony in soil and its availability to plants. *Chemosphere* **41** (11), 1791–1798. [https://doi.org/10.1016/S0045-6535\(00\)00037-0](https://doi.org/10.1016/S0045-6535(00)00037-0) (2000).
58. USEPA-United States Environmental Protection Agency. *Toxics Release Inventory. Doc. 745-R00-007* Washington (USEPA, 1979).
59. Tyenda, C. A., Torres, F. A. T. & Sullivan, D. W. Jr Antimony. In *Handbook on the Toxicology of Metals*. 23–40. (Academic Press, 2022). <https://doi.org/10.1016/B978-0-12-822946-0.00002-7>
60. Chang, S., McDonald-Buller, E., Kimura, Y., Yarwood, G., Neece, J., Russell, M. & Allen, D. Sensitivity of urban ozone formation to chlorine emission estimates. *Atmos. Environ.* **36** (32), 4991–5003. [https://doi.org/10.1016/S1352-2310\(02\)00573-3](https://doi.org/10.1016/S1352-2310(02)00573-3) (2002).
61. Kohlhammer, Y. & Heinrich, J. Chlorine, chlorination by-products and their allergic and respiratory health effects. *Curr. Respir. Med. Rev.* **3** (1), 39–47. <https://doi.org/10.2174/157339807779941839> (2007).
62. Gajbhiye, T. et al. SEM-EDS-based rapid measurement and size-fractionated speciation of airborne particulate matter and associated metals utilizing plant leaves. *Environ. Sci. Pollut. Res.* **31**, 47144–47156. <https://doi.org/10.1007/s11356-024-34222-9> (2024).
63. Nikum, R. D. & Nehete, J. Y. Review on traditionally medicinal importance, morphology, phyto-chemistry and pharmacological activities of Dalbergia Sisso. *Int. J. Pharmacogn.* **8** (8), 329–337 (2021).
64. Shah, S., Shah, S.M., Ullah, A., Ali, U., Khan, M.N., Sultana, S. & Etim, M. Light and scanning electron microscopic investigation of selected taxa of fabaceae and its utilization for taxonomic classification. *J. Xi'an Shiyu Univ.* **19** 262–272 (2023).
65. Begum, A., Rahman, M. O. & Begum, M. Stomatal and trichome diversity in Senna Mill. From Bangladesh. *Bangladesh J. Plant. Taxon.* **21** (1), 43 (2014).
66. Baesso Moura, B. et al. Comparing different methodologies to quantify particulate matter accumulation on plant leaves. *Urban Sci.* **8**, 125. <https://doi.org/10.3390/urbansci8030125> (2024).
67. Yin, H., Mu, S., Zhao, L., Qi, X. & Pan, X. Microscopic morphology and elemental composition of size distributed atmospheric particulate matter in Urumqi, China. *Environ. Earth Sci.* **69**, 2139–2150. <https://doi.org/10.1007/s12665-012-2043-y> (2013).
68. Zeb, B. et al. On the morphology and composition of particulate matter in an urban environment. *Aerosol Air Qual. Res.* **18** (6), 1431. <https://doi.org/10.4209/aaqr.2017.09.0340> (2018).
69. Goel, V. et al. Insights into coarse particle optics based on field evidence of particle morphology, chemical composition and internal structure. *Atmos. Environ.* **232**, 117338. <https://doi.org/10.1016/j.atmosenv.2020.117338> (2020).
70. Telloli, C., Chicca, M., Leis, M. & Vaccaro, C. Fungal spores and pollen in particulate matter collected during agricultural activities in the Po Valley (Italy). *J. Environ. Sci.* **46**, 229–240. <https://doi.org/10.1016/j.jes.2016.02.014> (2016).
71. Satsangi, P. G. & Yadav, S. Characterization of PM_{2.5} by X-ray diffraction and scanning electron microscopy–energy dispersive spectrometer: Its relation with different pollution sources. *Int. J. Environ. Sci. Technol.* **11**, 217–232. <https://doi.org/10.1007/s13762-012-0173-0> (2014).
72. Bora, J., Deka, P., Bhuyan, P., Sarma, K. P. & Hoque, R. R. Morphology and mineralogy of ambient particulate matter over Mid-brahmaputra Valley: Application of SEM–EDX, XRD, and FTIR techniques. *SN Appl. Sci.* **3**, 1–15. <https://doi.org/10.1007/s42452-020-04117-8> (2021).
73. Pipal, A. S., Kulshrestha, A. & Taneja, A. Characterization and morphological analysis of airborne PM_{2.5} and PM₁₀ in Agra located in north central India. *Atmos. Environ.* **45** (21), 3621–3630. <https://doi.org/10.1016/j.atmosenv.2011.03.062> (2011).
74. Kwak, M.J., Lee, J.K., Park, S., Kim, H., Lim, Y.J., Lee, K.A. & Woo, S. Y. Surface-based analysis of leaf microstructures for adsorbing and retaining capability of airborne particulate matter in ten woody species. *Forests*, **11** (9), 946. <https://doi.org/10.3390/f11090946> (2020).
75. Srivastava, A., Jain, V. K. & Srivastava, A. SEM-EDX analysis of various sizes aerosols in Delhi India. *Environ. Monit. Assess.* **150** (1), 405–416. <https://doi.org/10.1007/s10661-008-0239-0> (2009).
76. Rana, S., Saxena, M. R. & Maurya, R. K. A review on morphology, nanostructure, chemical composition, and number concentration of diesel particulate emissions. *Environ. Sci. Pollut. Res.* **29** (11), 15432–15489. <https://doi.org/10.1007/s11356-021-15999-5> (2022).
77. Gupta, P. et al. Exposure to respirable and fine dust particle over North-Central India: Chemical characterization, source interpretation, and health risk analysis. *Environ. Geochem. Health.* **42**, 2081–2099. <https://doi.org/10.1007/s10653-019-00461-w> (2020).
78. Novela, R. J. et al. Chemical characterization of fine particulate matter, source apportionment and long-range transport clusters in Thohoyandou, South Africa. *Clean. Air J.* **30** (2), 1–12. <https://doi.org/10.17159/caj/2020/30/2.8735> (2020).
79. Mustafa, N. N. & Raine, R. R. Electron microscopy investigation of particulate matter from a dual fuel engine. *Aerosol Sci. Technol.* **43** (9), 951–960. <https://doi.org/10.1080/02786820903067210> (2009).

Acknowledgements

This research work was funded by Institutional Fund Project under grant no. (IFPIP: 698-130-1443). The authors gratefully acknowledge technical and financial support provided by the Ministry of Education and King Abdulaziz University, DSR, Jeddah, Saudi Arabia. We also acknowledge the anonymous reviewers for their valuable suggestions that helped improve the final version of this manuscript.

Author contributions

A.T.: Conceptualization, Data curation, Writing-Original draft, Writing-review & editing, Formal Analysis, Visualization. T.G.: Conceptualization, Writing-review & editing. M.P.: Writing-review & editing. K.A.: Formal analysis. S.N.: Formal analysis. S.M.: Formal analysis. D.P.: Formal analysis, R.D.: Writing-review & editing. T.G.M.: Review & editing. M.Z.: Writing-review & editing. A.Z.: Writing-review & editing. K.M.A.: Writing-review & editing. K.R.A.: Writing-review & editing S.K.P.: Supervision, Conceptualization, Validation, Writing-review & editing.

Funding

This research work was funded by Institutional Fund Project under grant no. (IFPIP: 698-130-1443). The authors gratefully acknowledge technical and financial support provided by the Ministry of Education and King Abdulaziz University, DSR, Jeddah, Saudi Arabia.

Declarations

Competing interests

The authors declare no competing interests.

Ethics approval and consent to participate

We, the authors of this manuscript, hereby declare that the content presented in this research article is original and has not been published elsewhere. All contributions made by co-authors are appropriately acknowledged.

Additional information

Supplementary Information The online version contains supplementary material available at <https://doi.org/10.1038/s41598-024-84552-4>.

Correspondence and requests for materials should be addressed to R.D. or S.K.P.

Reprints and permissions information is available at www.nature.com/reprints.

Publisher's note Springer Nature remains neutral with regard to jurisdictional claims in published maps and institutional affiliations.

Open Access This article is licensed under a Creative Commons Attribution-NonCommercial-NoDerivatives 4.0 International License, which permits any non-commercial use, sharing, distribution and reproduction in any medium or format, as long as you give appropriate credit to the original author(s) and the source, provide a link to the Creative Commons licence, and indicate if you modified the licensed material. You do not have permission under this licence to share adapted material derived from this article or parts of it. The images or other third party material in this article are included in the article's Creative Commons licence, unless indicated otherwise in a credit line to the material. If material is not included in the article's Creative Commons licence and your intended use is not permitted by statutory regulation or exceeds the permitted use, you will need to obtain permission directly from the copyright holder. To view a copy of this licence, visit <http://creativecommons.org/licenses/by-nc-nd/4.0/>.

© The Author(s) 2025